Soft Matter

PAPER

Hydrodynamic capture of microswimmers into sphere-bound orbits†

Cite this: *Soft Matter*, 2014, **10**, 1784

Daisuke Takagi,[ab] Jérémie Palacci,[c] Adam B. Braunschweig,[d] Michael J. Shelley[b] and Jun Zhang[bc]

Received 7th November 2013
Accepted 20th January 2014

DOI: 10.1039/c3sm52815d

www.rsc.org/softmatter

Self-propelled particles can exhibit surprising non-equilibrium behaviors, and how they interact with obstacles or boundaries remains an important open problem. Here we show that chemically propelled micro-rods can be captured, with little change in their speed, into close orbits around solid spheres resting on or near a horizontal plane. We show that this interaction between sphere and particle is short-range, occurring even for spheres smaller than the particle length, and for a variety of sphere materials. We consider a simple model, based on lubrication theory, of a force- and torque-free swimmer driven by a surface slip (the phoretic propulsion mechanism) and moving near a solid surface. The model demonstrates capture, or movement towards the surface, and yields speeds independent of distance. This study reveals the crucial aspects of activity–driven interactions of self-propelled particles with passive objects, and brings into question the use of colloidal tracers as probes of active matter.

Biological systems demonstrate that the presence of obstacles, which could be a solid surface or a group of cells, profoundly affects the autonomous movement of microscopic swimmers. Motile cells can aggregate[1] and move in circles on surfaces,[2] reverse directions when they are spatially constricted,[3] and migrate preferentially through an array of V-shaped funnels.[4] Bacteria may enhance the diffusivity of surrounding tracer particles,[5,6] drive ratchets into rotary motion,[7,8] and form large rotating structures through collective movements.[9] Interactions between bacteria and the physical environment are widely documented but complicated because, in addition to possible collisional[10] and hydrodynamic[11] effects, there are unknown responses associated with motile behavior.

Recent technological advances have enabled the fabrication of synthetic microswimmers that convert chemical energy into directional motion.[12–16] Their movements can collectively drive the system out of equilibrium and exhibit large-scale phenomena such as schooling[17] and clustering.[18,19] Studying the dynamics of self-propelled particles is important because they may have useful ensemble properties, inspire new designs for smart materials, and find many applications including microfluidic mixing devices and cargo transport.[20–22]

Synthetic swimmers are arguably simpler than bacteria and offer insight into the effects of obstacles and confinement on self-propelled particles. Here we employ a widely studied system consisting of gold–platinum (Au–Pt) segmented rods immersed in an aqueous hydrogen peroxide solution (H_2O_2).[12] Previous studies propose that these rods propel themselves *via* self-electrophoresis, which generates a slip flow along the rod surface.[23,24] Recent studies show that synthetic swimmers interact with rigid boundaries, say by sliding along walls[25,26] and enhancing the diffusivity of tracer particles,[27] but the mechanisms of the interactions remain unclear.

Here we show that self-propelled Au–Pt rods are captured and orbit closely, with little decrease in their speed, around solid passive spheres resting on a solid substrate (Fig. 1). We show that this interaction between rod and sphere is short range, occurs for spheres of various materials and sizes, including spheres below the rod length. While the spheres appear to attract the rods, the Stokesian fluid environment precludes any net force or torque being exerted upon them. We explain some of these observations using a simple model, based on lubrication theory, of a swimming particle moving near a wall and propelled by a surface slip. This is a suitable assumption for modeling the motion of phoretic swimmers and motile ciliates.[28]

Results and Discussion

Experimental system

We fabricate Au–Pt rods with length $l = 2 \pm 0.2$ μm and diameter 0.39 ± 0.04 μm following the method of

[a]*Department of Mathematics, University of Hawaii at Manoa, Honolulu, Hawaii 96822, USA. E-mail: dtakagi@hawaii.edu*

[b]*Applied Math Lab, Courant Institute, New York University, New York, New York 10012, USA. E-mail: shelley@cims.nyu.edu; jun@cims.nyu.edu*

[c]*Department of Physics, New York University, New York, New York 10003, USA. E-mail: jp153@nyu.edu*

[d]*Department of Chemistry, University of Miami, Coral Gables, Florida 33146, USA. E-mail: a.braunschweig@miami.edu*

† Electronic supplementary information (ESI) available. See DOI: 10.1039/c3sm52815d

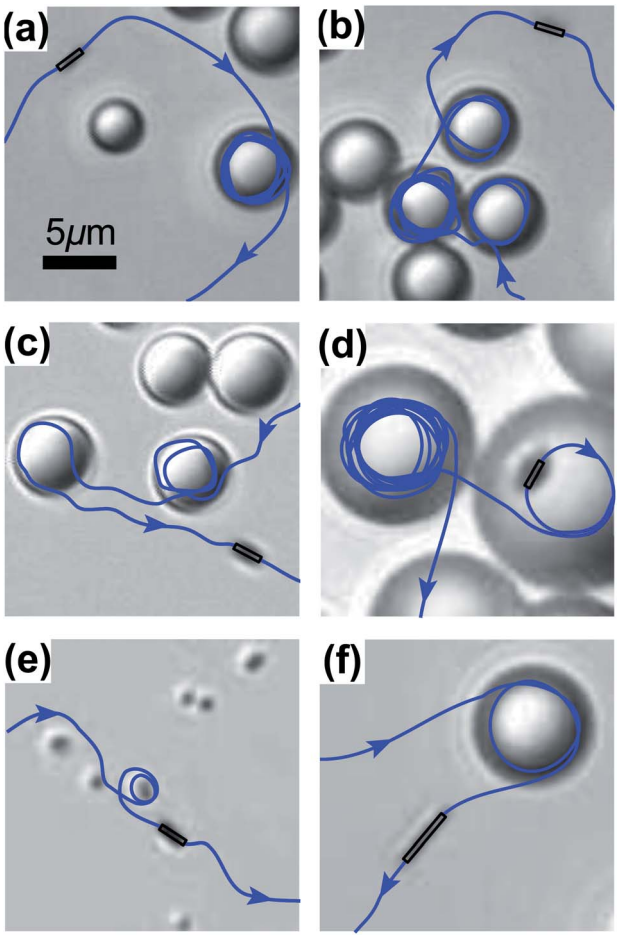

Fig. 1 Sample trajectories of self-propelled rods orbiting around passive spheres. The spheres have diameter ~6 μm in (a–c), 11 and 14 μm in (d), 1 μm in (e), and 9 μm in (f), and are made of various materials (see main text). The rod length is 2 μm in (a–e) and 4 μm in (f). The speed of the rods is on the order of 20 μm s^{-1}.

electrochemical deposition in anodic aluminum oxide membranes.[29,30] They are immersed in ~15% H_2O_2 containing passive spheres, with diameters of 1 to ~100 μm. Due to gravity, both rods and spheres remain close to, and move along, the plane of the microscope slide. The positions of the rods and spheres are tracked using optical microscopy (Nikon Eclipse 80i, 40×), a digital camera (Lumenera Infinity 1–3), and image analysis (ImageJ and Matlab). The spheres are transparent so each rod can be tracked even when it is underneath them. In the absence of passive spheres, the moving rods turn, flip, and disperse over time as reported previously.[31]

Capture of self-propelled rods by passive spheres. The presence of passive spheres significantly alters the trajectories of self-propelled rods (Fig. 1 and Movie S1†). When a self-propelled rod encounters a sphere, it typically orbits around it (Fig. 1a). The rod can move around a succession of spheres and either continue to turn in the same sense (Fig. 1b) or switch the handedness of its circular orbit (Fig. 1c).

This phenomenon of rods orbiting around spheres occurs across a wide range of materials and sizes (Fig. 1d–f). We have used rods of different lengths (1, 2 and 4 μm) and spheres of various diameters (1, 3, 6, 9, 11, 14, 20 and 125 μm) made of glass, polymerized 3-(trimethoxysilyl)propyl methacrylate (TPM),[32] poly(methyl methacrylate) (PMMA), and polystyrene. These materials have different surface properties but this does not affect the capture effect. Self-propelled rods are captured by all spheres that remain close to the substrate by gravity, including glass beads as small as 1 μm in diameter (half the rod length in Fig. 1e; see Movie S2†). On a sheet of mica with cleavages which act as nearly vertical walls on a horizontal surface, the rods are transitorily trapped along the walls in a similar fashion to what has been reported before.[25] This demonstrates that the rods are captured by confining walls with a variety of shapes and materials, and suggests a physical mechanism for the capture effect.

Capture phenomenon with no additional drag. Self-propelled rods nearly maintain their typical speed while they orbit around spheres (Fig. 2). While a rod is captured, it remains in a narrow fluid region between the sphere and the horizontal glass substrate, and shows little change in speed in this confined space. Given that the rod speed depends on the local fuel concentration,[31] this points to uniform fuel near the sphere as in the bulk.

Do spheres also rotate while a rod orbits around them? To answer this we use inert TPM spheres with an embedded piece of hematite acting as a marker.[33] The rotational diffusion of the sphere is slow compared to the orbiting time of the rod, and the orientation of the marker remains apparently unchanged (Fig. 3 and Movie S3†). A Fourier frequency analysis of sphere displacements shows that while the sphere does fluctuate slightly because of Brownian motion, there is also an oscillation of the sphere at the same frequency as the rod orbital motion. However, this effect is small and not discussed in this paper.

The nearly constant rod speed and the lack of sphere rotation suggest that the rods hardly experience any additional drag

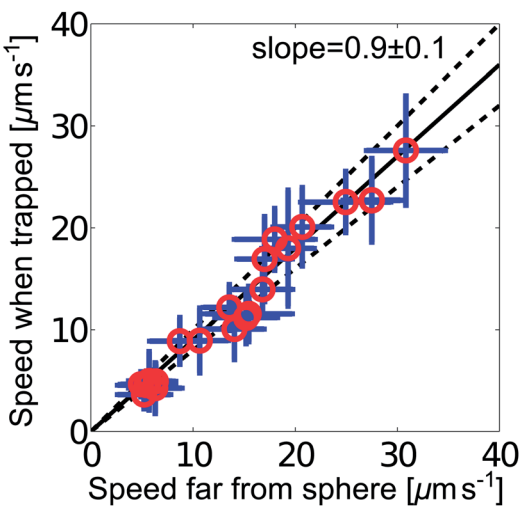

Fig. 2 While self-propelled rods are trapped, they move at speeds comparable to when they are far away from spheres. Symbols and error bars respectively show the temporal mean and standard deviation in speed of each rod. Solid and dashed lines have slopes 0.9 ± 0.1. Data collected at different H_2O_2 concentrations and over many events.

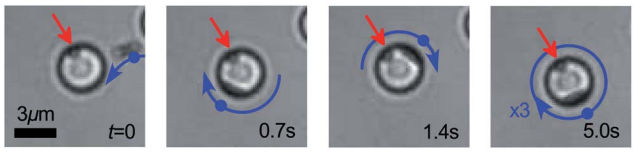

Fig. 3 Image sequence of a solid sphere of diameter ~3 μm which hardly rotates while a 2 μm-long self-propelled rod orbits around it. Red arrows point to a marker on the sphere. Blue dots and arrows show the location and direction of motion of the orbiting rod.

despite moving close to the solid spheres. This direct experimental evidence supports the hypothesis that the rods generate a local propulsive flow along their surface[23,24] as examined in our theory below. The theory helps to interpret the three observations that self-propelled rods are captured by spheres, the rods maintain their speed, and the spheres are unaffected by the rods.

Tentative scenarios of capture. One possible mechanism of trapping might be the exhaustion of the chemical fuel in the confined region beneath the sphere. However, in our previous work,[31] we showed that the swimming speed depends linearly on the fuel concentration. Here, we find that the capture of the rod scarcely diminishes its speed (Fig. 2). This suggests that the fuel concentration beneath the sphere is nearly that in the bulk. Further, while there is constant depletion of fuel at the rod surface, the rod is also moving away and hence leaves behind the depleted region for recovery. Any fixed region is revisited by the rod after an orbital timescale $\tau_{orb} \sim L/U$, where $L \sim 6$ μm is the typical sphere diameter and $U \sim 20$ μm s^{-1} the typical speed. The time scale needed to restore the fuel level by diffusion is $\tau_{dif} \sim L^2/D$, where $D \sim 10^3$ μm^2 s^{-1} is the fuel diffusivity. The fuel level in the space confined by the sphere and the substrate may seem harder to recover compared to that for an open region, but diffusion that takes places at the molecular level should give rise to the same timescale. The time scale for diffusion is 10 times faster than that for rod translation, giving the Peclet number $\tau_{dif}/\tau_{orb} = UL/D \sim 0.1$. The small Peclet number signifies that, as the rod returns to the same spot, diffusion has already restored the fuel level to that in the bulk. Hence it appears that the fuel consumption by the moving rods is not playing a determinant role in their trapping next to the spheres.

There are other possible mechanisms of trapping. Long-range hydrodynamic effects may enable swimmers to approach a solid surface as shown for a point particle with an extensile force dipole (pusher),[1,34] though our rods experience only short-range interactions with spheres as confirmed below. The rods are slightly curved and tend to move in curved paths with typical curvature $\kappa \sim 0.12$ μm^{-1},[31] so they could slide along flat[35] and curved surfaces with curvature much less than κ.[36] However, we observe rods orbiting around spheres with diameter as small as 1 μm, which has curvature much greater than κ.

In our interpretation, aside from thermal fluctuations, the rods move towards a surface because the local flow field is modified by its presence. This is demonstrated in a simplified model based on lubrication theory. Such a motion would not occur for an object towed by a force parallel to a solid boundary due to the symmetry and time-reversibility of Stokes flow. The key ingredient in our model is a prescribed slip on the swimming body, which captures a phoretic propulsion mechanism. By assuming a suitable slip velocity, the model predicts the swimmer's speed and trajectory as well as the forces acting on the surface, which are all in agreement with our experimental observations as discussed below.

Short-range hydrodynamic capture

Mathematical model. While our experimental system is three dimensional with curved boundaries (Fig. 4a), for simplicity we consider a two-dimensional swimmer moving above a flat immobile wall (Fig. 4b). Thermal fluctuations are neglected. We adopt a Cartesian coordinate system (x and y) in the reference frame that translates with the swimmer along the wall, where x is scaled by a half of the length of the swimming body $l/2$ and y is scaled by a typical distance H between the swimmer and the wall. The wall is represented by $y = 0$ and translates to the right with speed U, where all speeds are scaled by a typical slip velocity V on the swimmer. The wall-facing surface of the swimmer is represented by $y = h$ with $h = h_0(1 + mx)$, $-1 \le x \le 1$, where h_0 is a re-scaled distance from the wall to the center of the swimmer and m is a re-scaled slope of the swimmer relative to the wall. Note that $m = 1$ corresponds to the front end of the swimmer (the left end in Fig. 4b) hitting the wall.

Lubrication theory describes the fluid flow between the swimmer and the wall, provided that both the Reynolds number of the flow and $\delta = H/l$ are small. In our experiments we estimate δ to be in the order of 10^{-1}. Our approach is similar to that

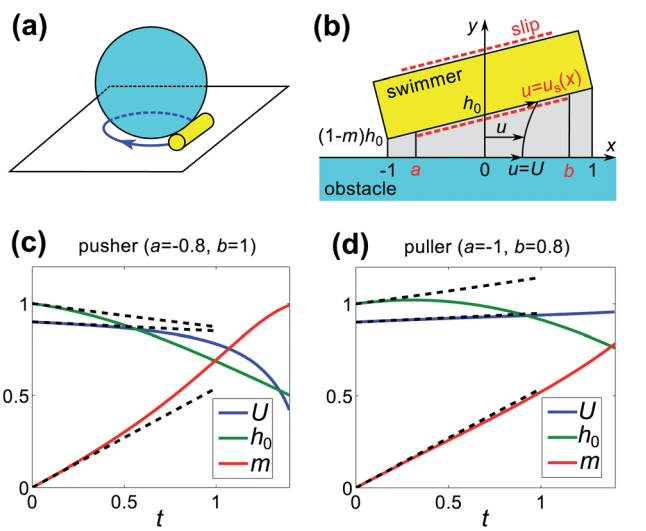

Fig. 4 (a) Sketch of a rod orbiting around a sphere on a horizontal surface. (b) Theoretical configuration of a swimming body near a rigid wall in the reference frame of the swimmer. The wall approximates the local surface of the sphere and translates to the right. Dashed lines show the region of fluid slip. (c and d) Predictions for the swimming speed U, distance h_0 away from the wall, and re-scaled slope m of a swimmer with fluid slipping over (c) $-0.8 < x < 1$ and (d) $-1 < x < 0.8$. Dashed lines show the early-time regime (eqn (5)–(7)).

used in modeling of crawling snails.[37] The flow is primarily in the x direction and governed by $d^2u/dy^2 = dp/dx$, where u is the flow speed, p is the pressure scaled by $\mu VH/l^2$, and μ is the dynamic viscosity of the fluid. The solution is given by

$$u = \frac{1}{2}\frac{dp}{dx}y(y-h) + \frac{y}{h}(u_s - U) + U, \quad (1)$$

which satisfies the boundary conditions $u = U$ on $y = 0$ and $u = u_s(x)$ on $y = h$. Substituting eqn (1) into the condition $\partial h/\partial t + (\partial/\partial x)\int_0^h u dy = 0$ that the mass is conserved, we obtain

$$\frac{dp}{dx} = \frac{6}{h^3}\left[\dot{h}_0 x(2+mx) + \dot{m}h_0x^2 + h(U+u_s) - 2q_0\right]. \quad (2)$$

Here q_0 is a constant, which is obtained by integrating eqn (2) with respect to x and requiring that $p = 0$ at the ends $x = \pm 1$. Eqn (1) and (2) are used to convert the conditions that the swimmer is force- and torque-free,

$$\int_{-1}^{1}\frac{du}{dy}|_{y=h}dx = \int_{-1}^{1}p dx = \int_{-1}^{1}xp dx = 0, \quad (3)$$

into a system of ordinary differential equations.

There are three predictions of our model which are all in agreement with our experimental observations. One prediction is the swimming speed

$$U = \frac{m}{\ln\left(\frac{1+m}{1-m}\right)}\int_{-1}^{1}\frac{u_s(x)dx}{1+mx}, \quad (4)$$

which is independent of the distance h_0 between the swimmer and the wall. This agrees with our observation that the rods nearly maintain their speed regardless of their proximity to the spheres (Fig. 2). Another prediction is that the total tangential and normal forces exerted on the wall are both zero. This is consistent with minimal force and torque exerted on the spheres (Fig. 3). Finally, the trajectories of rods orbiting around spheres (Fig. 1) correspond to swimmers approaching the wall, which is predicted for swimmers with fluid slip on most of their body as considered below.

We consider a simple class of swimmers with constant slip $u_s = 1$ on a portion of their surface $a < x < b$ and no slip $u_s = 0$ elsewhere. This assumption is motivated by the previous hypothesis that the rods generate a local flow on their surface, and offers important insight into the effect of fluid slip on the swimmer trajectory near a rigid boundary. At early times, a swimmer that is initially parallel to the wall with $h_0 = 1$ evolves according to the asymptotic solutions

$$U \sim \frac{1}{2}(b-a) - \frac{15}{32}\left(b^2-a^2\right)\left(b-a-\left(b^3-a^3\right)\right)t, \quad (5)$$

$$h_0 \sim 1 - \frac{3}{8}\left(b^2-a^2\right)t, \quad (6)$$

$$m \sim \frac{15}{8}\left(b-a-\left(b^3-a^3\right)\right)t, \quad (7)$$

valid to second order in time. Eqn (7) shows that, regardless of the exact region of slip, all swimmers with fluid slipping on a majority of their surface orient towards the wall. Temporal changes in m, h_0, and U are shown for two typical swimmers with slip everywhere except either near its front or back end of the swimmer (Fig. 4c and d). In both cases, the swimmer approaches the wall, and its changes in speed can be related to the relative position of its no-slip region to the wall. While this simple model does not allow for a quantitative comparison with the experiments, it demonstrates that self-propelled rods can be captured by spheres without applying any net force or torque on them as in our experiments.

Consequences and limitations of the model. Our approach extends previous theories on swimmers moving near a solid wall. Swimmers represented by point particles move closer to the wall if they are 'pushers' while they move away if they are 'pullers'.[1,34] Our model shows that phoretic swimmers, represented by a surface with fluid slipping on a majority of their body, remain very close to the wall regardless of the region of fluid slip.

In our model the front end of the swimmer approaches the wall in finite time (Fig. 4c and d). In contrast, non-swimmers or objects driven by an external force would require an infinite time to reach the wall. Our model demonstrates that fluid slip on the swimmer has a strong effect on its interactions with solid surfaces, though the effect may be modified by thermal fluctuations in our experiments.

Our model does not account for the existence of the substrate as an additional wall. However, we expect that the substrate has no major effect on the lateral interactions between the self-propelled rods and spheres. Observations of rods swimming in the bulk fluid and interacting freely with suspended obstacles are desirable for testing this hypothesis but they are extremely challenging because of the large density contrast between our rods and the surrounding fluid. Curiously though, the interaction of the rods with the substrate does provide some indirect support for our conception of rod–sphere interactions. In our previous work[31] on the diffusion of slightly curved swimming rods, we observed that their effective distance h_0 above the substrate is noticeably smaller than the computed sedimentation height of passively diffusing rods. The distance h_0 is deduced (see Fig. 2b of Takagi *et al.*[31]) from the flipping frequency of the rod between two side-laying configurations of the rod as they move along the substrate. This suggests that there is an additional effect beyond gravity which draws the rod closer to the substrate.

To verify experimentally that only short-range interactions occur between self-propelled rods and passive spheres, we consider the distribution of rod positions relative to the center of a nearby sphere (Fig. 5a). This is measured by sampling the distance from a given rod to the nearest sphere over time, excluding cases where the rod has multiple spheres within three sphere radii. For passive rods in water, the density is nearly uniform everywhere except below the sphere, where the density decreases to zero. Active rods also have a uniform distribution away from the sphere, but in contrast to passive rods now show a sharp peak below the sphere. These features for self-propelled rods are consistent with the hypothesis of capture through short-range interactions. Further, hydrodynamic interactions

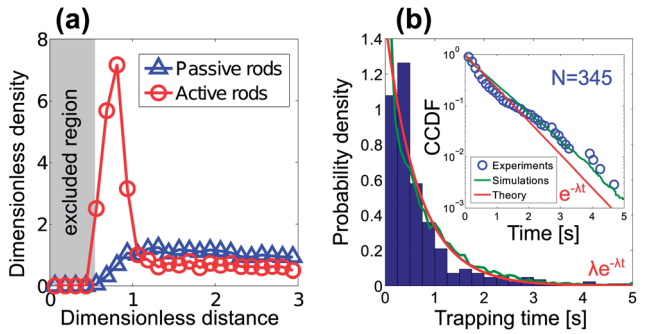

Fig. 5 (a) Experimental data of the effective density of a suspension of rods, scaled by the expectation if the rods were distributed uniformly. This is plotted against the distance from the lowest point of a sphere in units of the sphere radius 2.8 μm, based on over 4000 measurements of the distance over time. Below the sphere, the density of passive rods falls while the density of self-propelled rods peaks. Density of zero is shown in the excluded region where the rods are physically unable to enter. (b) Normalized histogram of trapping times of self-propelled rods orbiting around spheres. Inset shows the complementary cumulative distribution function (ccdf) denoting the probability of rods remaining trapped beyond a specified time. Red curves are exponential distributions with rate parameter $\lambda = 1.5\ s^{-1}$. Green curves are simulated trapping times (see main text).

induced by the rod's propulsive mechanism enable the spheres to capture self-propelled rods but not passive ones.

Capture time statistics. While our deterministic model predicts that swimmers move closer to a solid surface, fluctuations may cause them to move away or remain at some characteristic distance. In our experiments the trapping is transitory, and we observe that the trapping times are typically less than 5 seconds and have an exponential distribution with decay rate $\lambda \sim 1.5\ s^{-1}$ (Fig. 5b). The trapping time-scale (λ^{-1}) is comparable to the time-scales of rotational diffusion and duration between stochastic flips ($\sim 1s$).[31]

In rare instances, the rods remain trapped on the order of minutes. Highly curved rods that move in small circles tend to either remain trapped for relatively long times or are hardly trapped, depending on whether they approach a sphere with the trajectory curving towards or away from the sphere, respectively. One possible interpretation of this is that the rods are curved towards the sphere while they are trapped until thermal fluctuations flip them over[31] and enable them to escape.

To study the effect of thermal fluctuations on the trapping time, we carried out simple simulations of our model with the added effect of rotational Brownian motion. Consider a swimmer with fluid slip over 90% of its body length $l = 2$ μm ($a = -0.9$, $b = 0.9$) moving at speed $U = 20\ \mu m\ s^{-1}$ at a typical distance $H \sim 0.2$ μm from the wall. We simulate the orientation angle θ of 10 000 swimmers which are initially parallel to a wall. The angle evolves according to the Langevin equation

$$\theta(t + \Delta t) = \theta(t) + \Omega \Delta t + \sqrt{2 D_r \Delta t} X, \quad (8)$$

where $\Omega \sim 3/s$ is the typical rotation rate estimated using eqn (7), $D_r = 1/s$ is the rotational diffusion constant, and X is a random variable with normal distribution. This shows that the trapping time, defined as the time it takes for the angle to decrease to a threshold value $-\pi/9$, is exponentially distributed in agreement with our experimental data (Fig. 5b). The relative residence times of trapped *vs.* untrapped particles would then yield the relative densities in Fig. 5a. While thermal fluctuations interacting with the capture effect seem to explain the basic mechanisms at work, a more predictive theory should include swimmer geometry and detailed chemistry.

Conclusion

Suspensions of self-propelled and passive particles reveal new activity–driven interactions in active matter. Swimmers with an effective slip on a majority of their surface, including phoretic particles[23,24] and motile ciliates,[28] move stealthily without much disturbance to the surrounding fluid and objects within it. Still, the swimmers themselves are captured by solid boundaries and can accumulate in spatially constricted regions, unlike passive particles. The different responses to the presence of obstacles could be exploited, for example, to separate swimmers and passive particles.[38,39] However, such an application remains speculative because swimmer–particle interactions may have profound and long-term effects which require further exploration. Our results also bring into question the use of colloidal tracers as probes in out-of-equilibrium systems, as for example in measuring the effective temperature of an active bath.[5,6,27] The tracers may not fully capture the complex swimmer movements and enhanced fluid mixing which could emerge in concentrated suspensions.

Acknowledgements

We thank S. Sacanna for the hematite-encapsulating spheres used in this study. We acknowledge support from NSF (NYU MRSEC DMR-0820341, MRI-0821520, DMR-0923251, DMS-0920930), DOE (DE-FG02-88ER25053), and AFOSR (FA-9550-13-1-0188).

References

1 A. P. Berke, L. Turner, H. C. Berg and E. Lauga, *Phys. Rev. Lett.*, 2008, **101**, 38102.
2 E. Lauga, W. R. DiLuzio, G. M. Whitesides and H. A. Stone, *Biophys. J.*, 2006, **90**, 400–412.
3 L. Cisneros, C. Dombrowski, R. E. Goldstein and J. O. Kessler, *Phys. Rev. E: Stat., Nonlinear, Soft Matter Phys.*, 2006, **73**, 030901.
4 P. Galajda, J. Keymer, P. Chaikin and R. Austin, *J. Bacteriol.*, 2007, **189**, 8704–8707.
5 X. L. Wu and A. Libchaber, *Phys. Rev. Lett.*, 2000, **84**, 3017–3020.
6 K. C. Leptos, J. S. Guasto, J. P. Gollub, A. I. Pesci and R. E. Goldstein, *Phys. Rev. Lett.*, 2009, **103**, 198103.
7 R. Di Leonardo, L. Angelani, D. Dell'Arciprete, G. Ruocco, V. Iebba, S. Schippa, M. P. Conte, F. Mecarini, F. De Angelis and E. Di Fabrizio, *Proc. Natl. Acad. Sci. U. S. A.*, 2010, **107**, 9541–9545.

8 A. Sokolov, M. M. Apodaca, B. A. Grzybowski and I. S. Aranson, *Proc. Natl. Acad. Sci. U. S. A.*, 2010, **107**, 969–974.
9 J. Schwarz-Linek, C. Valeriani, A. Cacciuto, M. E. Cates, D. Marenduzzo, A. N. Morozov and W. C. K. Poon, *Proc. Natl. Acad. Sci. U. S. A.*, 2012, **109**, 4052–4057.
10 V. Kantsler, J. Dunkel, M. Polin and R. E. Goldstein, *Proc. Natl. Acad. Sci. U. S. A.*, 2013, **110**, 1187–1192.
11 K. Drescher, J. Dunkel, L. H. Cisneros, S. Ganguly and R. E. Goldstein, *Proc. Natl. Acad. Sci. U. S. A.*, 2011, **108**, 10940–10945.
12 W. F. Paxton, K. C. Kistler, C. C. Olmeda, A. Sen, S. K. St. Angelo, Y. Cao, T. E. Mallouk, P. E. Lammert and V. H. Crespi, *J. Am. Chem. Soc.*, 2004, **126**, 13424–13431.
13 S. Fournier-Bidoz, A. C. Arsenault, I. Manners and G. A. Ozin, *Chem. Commun.*, 2005, 441–443.
14 J. G. Gibbs and Y. P. Zhao, *Small*, 2009, **5**, 2304–2308.
15 S. J. Ebbens and J. R. Howse, *Soft Matter*, 2010, **6**, 726–738.
16 S. Sengupta, M. E. Ibele and A. Sen, *Angew. Chem., Int. Ed.*, 2012, **51**, 8434–8445.
17 M. Ibele, T. E. Mallouk and A. Sen, *Angew. Chem., Int. Ed.*, 2009, **48**, 3308–3312.
18 I. Theurkauff, C. Cottin-Bizonne, J. Palacci, C. Ybert and L. Bocquet, *Phys. Rev. Lett.*, 2012, **108**, 268303.
19 J. Palacci, S. Sacanna, A. P. Steinberg, D. J. Pine and P. M. Chaikin, *Science*, 2013, **339**, 936–940.
20 M. Pumera, *Chem. Commun.*, 2011, **47**, 5671–5680.
21 J. Wang and W. Gao, *ACS Nano*, 2012, **6**, 5745–5751.
22 D. Patra, S. Sengupta, W. Duan, H. Zhang, R. Pavlick and A. Sen, *Nanoscale*, 2013, **5**, 1273–1283.
23 Y. Wang, R. M. Hernandez, D. J. Bartlett, Jr, J. M. Bingham, T. R. Kline, A. Sen and T. E. Mallouk, *Langmuir*, 2006, **22**, 10451–10456.
24 J. L. Moran and J. D. Posner, *J. Fluid Mech.*, 2011, **680**, 31–66.
25 G. Volpe, I. Buttinoni, D. Vogt, H. J. Kümmerer and C. Bechinger, *Soft Matter*, 2011, **7**, 8810–8815.
26 S. Thutupalli, PhD thesis, University of Göttingen, Germany, 2011.
27 G. Mino, T. E. Mallouk, T. Darnige, M. Hoyos, J. Dauchet, J. Dunstan, R. Soto, Y. Wang, A. Rousselet and E. Clement, *Phys. Rev. Lett.*, 2011, **106**, 48102.
28 H. A. Stone and A. D. T. Samuel, *Phys. Rev. Lett.*, 1996, **77**, 4102–4104.
29 B. R. Martin, D. J. Dermody, B. D. Reiss, M. Fang, L. A. Lyon, M. J. Natan and T. E. Mallouk, *Adv. Mater.*, 1999, **11**, 1021–1025.
30 M. J. Banholzer, L. Qin, J. E. Millstone, K. D. Osberg and C. A. Mirkin, *Nat. Protocols*, 2009, **4**, 838–848.
31 D. Takagi, A. B. Braunschweig, J. Zhang and M. J. Shelley, *Phys. Rev. Lett.*, 2013, **110**, 038301.
32 S. Sacanna, W. T. M. Irvine, L. Rossi and D. J. Pine, *Soft Matter*, 2010, **7**, 1631–1634.
33 S. Sacanna, L. Rossi and D. J. Pine, *J. Am. Chem. Soc.*, 2012, **134**, 6112.
34 S. Spagnolie and E. Lauga, *J. Fluid Mech.*, 2012, **700**, 105–147.
35 S. van Teeffelen and H. Löwen, *Phys. Rev. E: Stat., Nonlinear, Soft Matter Phys.*, 2008, **78**, 020101.
36 S. van Teeffelen, U. Zimmermann and H. Löwen, *Soft Matter*, 2009, **5**, 4510–4519.
37 B. Chan, N. J. Balmforth and A. E. Hosoi, *Phys. Fluids*, 2005, **17**, 113101.
38 W. Yang, V. R. Misko, K. Nelissen, M. Kong and F. M. Peeters, *Soft Matter*, 2012, **8**, 5175–5179.
39 P. K. Ghosh, V. R. Misko, F. Marchesoni and F. Nori, *Phys. Rev. Lett.*, 2013, **110**, 268301.